

Spectrophotometric Study of the Equilibria between Nickel(II) Schiff-Base Complexes and Alkaline Earth or Nickel(II) Cations in Acetonitrile Solution[†]

Laura Carbonaro,* Mauro Isola, Piero La Pegna,[‡] and Lucio Senatore[‡]

Dipartimento di Chimica e Chimica Industriale, Via Risorgimento 35, I-56100 Pisa, Italy

Fabio Marchetti

Dipartimento di Ingegneria Chimica, dei Materiali delle Materie Prime e Metallurgia, Università Degli Studi di Roma "La Sapienza", via del Castro Laurenziano 7, I-00195 Roma, Italy

Received February 17, 1999

Adduct formation between $M(\text{ClO}_4)_2$ and nickel(II) complexes of tetradentate Schiff-base ligands ([NiL]) have been investigated in acetonitrile by means of UV–vis spectrophotometric analysis ($M^{2+} = \text{Mg}^{2+}, \text{Ca}^{2+}, \text{Sr}^{2+}, \text{Ba}^{2+}, \text{Ni}^{2+}$; [NiL] = [Ni(salen)] = [*N,N'*-ethylenebis(salicylideneiminato)]nickel(II), [Ni(salphen)] = [*N,N'*-phenylenebis(salicylideneiminato)]nickel(II), [Ni(salpren)] = [*N,N'*-propylenebis(salicylideneiminato)]nickel(II)). [NiL] complexes act as bidentate oxygen-donor ligands forming adducts of the type $[(\text{NiL})\text{M}]^{2+}$ and $[(\text{NiL})_2\text{M}]^{2+}$ whose general order of increasing stability was correlated to the dimensions of the M^{2+} cations. Complexes of general composition $2[\text{Ni}(\text{salen})] \cdot M(\text{ClO}_4)_2$ were isolated as powders in the solid state ($M = \text{Sr}, \text{Ca}, \text{Mg}$). X-ray structures of the crystalline complexes $\{[\text{Ni}(\text{salen})]_2\text{Ba}(\text{ClO}_4)_2(\text{thf})\}$ (**1**) (thf = tetrahydrofuran) and $\{[\text{Ni}(\text{salen})]_2\text{Ni}(\text{H}_2\text{O})_2(\text{ClO}_4)_2\}$ (**2**) are reported. **1** crystallizes in the space group $P2_1/c$ ($a = 10.995 \text{ \AA}$; $b = 20.830 \text{ \AA}$; $c = 19.567 \text{ \AA}$, $\beta = 116.94^\circ$) and **2** in $C2/c$ ($a = 10.3020 \text{ \AA}$; $b = 21.818 \text{ \AA}$; $c = 17.796 \text{ \AA}$; $\beta = 118.98^\circ$). Two [Ni(salen)] units act as oxygen bidentate ligands in both the compounds. The barium is coordinated to eight oxygen atoms in a distorted square antiprismatic geometry. An 8-fold coordination is completed by a molecule of tetrahydrofuran and two perchlorate anions acting as bi- and monodentate O-ligands, respectively. In **2**, the nickel atom, coordinated to two [Ni(salen)] complexes, has a distorted octahedral geometry and completes its coordination by linking two molecules of water.

Introduction

Much attention has been directed to host–guest chemistry for the analogy between enzyme–substrate complexes and host–guest complexes.¹ These latter may be defined as complexes between organic compounds that simulate the substrate selectivity of enzymes. A phenomenon described as “molecular recognition” derives from such interactions. A host may include a guest without covalent bond formation, giving rise to “inclusion complex formation”. The binding forces present in such complexes are recognized as van der Waals attractions, ion pairing, charge–dipole interaction, hydrogen bonding, metal ion to ligand attractions, and/or π acid to π base attraction, along with hydrophobic and solvent liberation driving forces.¹ In nature, these forces, although weak, allow the organization of the biological function, generating macromolecules.

Recently, the biological community has focused much of its interest on the understanding of the mechanism which governs the transmembrane flow of cationic species.² Among these, alkali (Na^+ and K^+) and alkaline earth (Ca^{2+} and Mg^{2+}) metals are of particular interest in living systems.³

The traditional approach to host–guest chemistry has been directed mainly to systems such as crown ethers,¹ although they

are unable to model metalloenzymes, in which the enzyme function is conditioned by the metal atom. On the contrary host systems, containing transition metals, have received much less attention.

The well-known structural and synthetic versatility of Schiff-base complexes^{4,5} provides an alternative route to design potential transition metal host systems. As early as 1925, work on salen derivatives has opened the possibility of producing a cavity, or lacuna, in the vicinity of the coordination site that contains the metal atom. Pendant arms bearing potential chelating groups which allow an opened cryptand ability toward metal guests have been introduced⁶ to improve the binding ability both in terms of selectivity and in terms of strength.

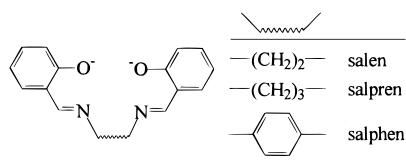
- (2) Stein, W. D. *Channels, Carriers and Pumps: An Introduction to Membrane Transport*; Academic Press: New York, 1990. Hille, B. *Ionic Channels of Excitable Membranes*, 2nd ed.; Sinauer Associates: Sunderland, MA, 1992.
- (3) Kendrick, M. J.; May, M. T.; Plinska, M. J.; Robinson, K. D. *Metals in Biological Systems*; Ellis Horwood Ltd.: Chichester, England, 1992; Chapters 3–5.
- (4) Sacconi, L.; Paoletti, P.; Del Re, G. *J. Am. Chem. Soc.* **1957**, *79*, 4062.
- (5) Yamada, S. *Coord. Chem. Rev.* **1966**, *1*, 415.
- (6) (a) Schepartz, A.; McDevitt, J. P. *J. Am. Chem. Soc.* **1989**, *111*, 5976. Boyce, M.; Clarke, B.; Cunningham, D.; Gallagher, J. F.; Higgins, T.; McArdle, P.; Cholchuin, M. N.; O'Gara, M. *J. Organomet. Chem.* **1995**, *498*, 241. Guerriero, P.; Tamburini, S.; Vigato, P. A. *Coord. Chem. Rev.* **1995**, *139*, 17. (b) Costes J. P.; Dahan F.; Laurent, J. P. *Inorg. Chem.* **1994**, *33*, 2738. Costes J. P.; Laurent J. P.; Chabert P.; Commenges G.; Dahan F. *Inorg. Chem.* **1997**, *36*, 656 and references therein.

[†] This work is part of the thesis of P.L.P. in partial fulfillment for the requirements of the degree of Philosophy Doctor of Chemical Sciences.

[‡] Deceased June 20, 1998.

(1) Maede, T. J.; Busch, D. H. In *Progress in Inorganic Chemistry*; Lippard S. J., Ed.; Wiley Interscience: New York, 1985; Vol. 33 and references therein.

Chart 1



However, in planning new systems, the knowledge of the behavior of the simpler parent complexes remains a useful, if not even indispensable, starting point.

In past years we have been interested in the field of molecular host–guest chemistry. In particular, we studied neutral systems derived from salicylaldehyde, in which a transition metal atom is incorporated into the structure of the host molecule.⁷ The ability of these complexes to capture alkali cations, giving rise to compounds which, in the crystalline state, correspond to molecular aggregates of stoichiometry 2:1 or 3:1, has been known for a long time.⁸ We faced the study of the phenomena in solution, also in relation to the interest that these polynuclear compounds cover in the catalysis field.⁹ Alkali metals in acetonitrile solution were found⁷ to form adducts 1:1 with transition metal Schiff-base complexes. In the present paper we extend such investigations to doubly charged metals dealing with the interaction in acetonitrile between five cations (Mg^{2+} , Ca^{2+} , Sr^{2+} , Ba^{2+} , and Ni^{2+}) and nickel(II) complexes of Schiff-base ligands having N_2O_2 donor sets (Chart 1).

Experimental Section

Physical Measurements. The IR spectra were recorded on a Perkin-Elmer 983 spectrophotometer. UV–vis spectra were recorded on a Perkin-Elmer Lambda 9 spectrophotometer. Ionic chromatographic analyses were performed by a Dionex Chromatograph S.4000. ¹H NMR spectra were recorded on a Varian Gemini 200. Plasma analyses were performed by a ICP/AES Varian Liberty 200.

Materials. [*N,N'*-Ethylenediimine]nickel(II)¹⁰ = [Ni(salen)], [*N,N'*-*o*-phenylenediimine]nickel(II)¹¹ = [Ni(salphen)], and [*N,N'*-propylenediimine]nickel(II)¹² = [Ni(salpren)] were prepared and purified according to the methods described in the literature. The solvents were carefully purified and dried by standard methods.

Caution! Perchlorate salts and complexes of metal ions are potentially explosive. Only small amounts should be dried and handled at a time.

Alkaline earth perchlorates (Aldrich products) were dried at 100 °C under vacuum. Ionic HPLC and plasma analysis confirmed the purity

of each salt. [Ni(CH₃CN)₆](ClO₄)₂ was prepared and purified according to the methods described in the literature¹³ and characterized by ¹H NMR and elemental and plasma analysis.

{[Ni(salen)]₂Ba(ClO₄)₂(thf)} (1) (thf = tetrahydrofuran) was prepared by diffusion of a thf solution (25 mL) of 0.1 mmol of [Ni(salen)] into a thf solution (25 mL) of 0.05 mmol of Ba(ClO₄)₂ under a N₂ atmosphere. After 24 h at 20 °C, X-ray quality red crystals of the product were filtered off, washed (thf), dried in a vacuum, and characterized. (Found: C, 40.63; H, 3.41; Ba, 12.92; N, 5.11; Ni, 10.99. C₃₆H₃₆BaCl₂N₄Ni₂O₁₃ requires C, 40.86; H, 3.43; Ba, 12.98; N, 5.29; Ni, 11.09.)

{[Ni(salen)]₂Ni(H₂O)₂}(ClO₄)₂ (2) was prepared similarly using thf solutions (25 mL) of 0.1 mmol of [Ni(salen)] and 0.1 mmol of Ni(ClO₄)₂·6H₂O. Red crystals suitable for an X-ray diffraction study were deposited in a period of 1 week. (Found: C, 40.60; H, 3.39; N, 5.61; Ni, 18.40. C₃₂H₃₂Cl₂N₄Ni₃O₁₄ requires C, 40.73; H, 3.42; N, 5.94; Ni, 18.66.)

The complexes of general composition 2[Ni(salen)]·M(ClO₄)₂ (M = Ba, Sr, Ca, Mg) precipitated from thf solutions as powders. Ionic HPLC on ClO₄[−] and plasma analysis on Ni²⁺ and M²⁺ confirmed the Ni/M²⁺ stoichiometric ratio. Elemental analysis gave results consistent with variable amounts of crystallization solvent molecules.

Equilibrium Constants. The stability constants and the molar absorptivities of the adducts have been determined by UV–vis absorption spectrophotometry under an inert atmosphere. The spectra of a series of constant concentration (~10^{−4} mol L^{−1}) solutions of nickel complexes [NiL] and increasing concentrations of M(ClO₄)₂ (up to 0.06 mol L^{−1}) were recorded with a Perkin-Elmer Lambda-9 spectrophotometer between 300 and 500 nm. The reactants were poured into the reaction vessel by a modified semiautomatic buret, Crison micro-BU2031. The reaction vessel and the cell compartment of the spectrophotometer were thermostated at 25 ± 0.1 °C. Total concentrations of reactants were determined by weight or by absorbance measurements by applying the Lambert-Beer law. Absorbance data as a function of the total concentrations of the reactants were computer-fitted to the appropriate equation, depending on the model to be tested, using a nonlinear least-squares program¹⁴ to obtain the equilibrium concentrations of the species in solution, their molar absorptivities at the selected wavelengths, and the equilibrium constants (for example, *K*₁ and *K*₂ of Scheme 1; see below). Global multiparametric analyses were performed on 10–25 wavelengths and 20–40 solutions for each system studied. Standard deviations from regression were less than 2.5 × 10^{−3}. Ion pairs involving ClO₄[−] anion were considered negligible in acetonitrile solution.¹⁵ Ion pairs were not taken into account in the numerical treatment of the experimental data for the [Ni(salen)]/Ba(ClO₄)₂ system in tetrahydrofuran solution, although in this solvent they might have some relevance. The rightness of this choice, which allowed a simplification of data analysis, was confirmed by the reliable results obtained. As any other external cation can interact with the starting complexes,⁷ ionic strength was not controlled. Its effect can be neglected for complexation reactions of neutral macrocyclic ligands with cations as long as the ionic strength is sufficiently low (0.05 mol L^{−1}).^{7a,16} In the present determinations, the ionic strength of the computer fitted experimental data was generally within this limit by far.

X-ray Diffraction Study. Some single crystals of 1 and 2 were selected in air and glued at the end of glass fibers. All the X-ray diffraction measurements have been done on a Siemens P4 four-circle diffractometer, equipped with graphite monochromatized Mo K α radiation ($\lambda = 0.71073 \text{ \AA}$). Low-temperature data collections have been performed by cooling the crystal with a cold nitrogen gas flow obtained by a Siemens LT-2A device. All data collections are made in $\omega/2\theta$ scan mode. Three standard reflections have been measured every 97

- (7) (a) Giacomelli, A.; Rotunno, T.; Senatore, L. *Inorg. Chem.* **1985**, *24*, 1303. (b) Giacomelli, A.; Rotunno, T.; Senatore, L.; Settambolo R. *Inorg. Chem.* **1989**, *28*, 3552.
- (8) (a) Gruber, S. J.; Harris, C. M.; Sinn E. *J. Chem. Phys.* **1968**, *49*, 2183. Sacconi, L.; Mani, F.; Bencini, A. In *Comprehensive Coordination Chemistry*; Wilkinson G., Ed.; Pergamon Press: Oxford, 1987; Vol 5, Chapter 50, pp 188–208 and references therein. (b) Armstrong, L. G.; Lip, H. C.; Lindoy, L. F.; McPartlin M.; Tasker, P. A. *J. Chem. Soc., Dalton Trans.* **1977**, 1771.
- (9) Gambarotta, S.; Fiallo, M. L.; Floriani, C.; Chiesi-Villa, A.; Guastini, C. *J. Chem. Soc., Chem. Commun.* **1982**, 503. Floriani, C.; Fiallo, M. L.; Chiesi-Villa, A.; Guastini, C. *J. Chem. Soc., Dalton Trans.* **1987**, 1367. Kurtz, D. N.; Shriver, D. F.; Klotz, I. M. *Coord. Chem. Rev.* **1977**, *24*, 145. Ibers, J. A.; Holm, R. H. *Science* **1980**, 209. Holm, R. H. *Chem. Soc. Rev.* **1981**, *10*, 455. Garner, C. D.; Harrison, P. M. *Chem. Ber.* **1982**, *113*. Thomson, A. J.; Thorneley, R. N. F. *Ibid.* **1982**, *113*. Gambarotta, S.; Arena, F.; Floriani, C.; Zanazzi, P. F. *J. Am. Chem. Soc.* **1982**, *104*, 5082. Gambarotta, S.; Urso, F.; Floriani, C.; Chiesi-Villa, A.; Guastini, C. *Inorg. Chem.* **1983**, *22*, 3966.
- (10) Pfeiffer, P.; Breith, E.; Lubbe, E.; Tsumaki, T. *Justus Liebig's Ann. Chem.* **1939**, 503, 84.
- (11) Pfeiffer P.; Hesse, T.; Pfützing, H.; Scholl, W.; Thielert, H. *J. Prakt. Chem.* **1937**, *149*, 217.
- (12) Holm, R. H. *J. Am. Chem. Soc.* **1961**, *83*, 4683.

- (13) Wickenden, A. E.; Krause, R. A. *Inorg. Chem.* **1965**, *4*, 404.
- (14) Ambrosetti R.; Ricci D.; Bianchini R. *Gazz. Chim. Ital.* **1997**, *127*, 567.
- (15) Libus, W.; Strzelecki, H. *Electrochim. Acta* **1970**, *15*, 703.
- (16) Izatt, R. M.; Zhang, X.; An, H.; Zhu, C. Y.; Bradshaw, J. S. *Inorg. Chem.* **1994**, *33*, 1007 and references therein.

Table 1. Crystal Data and Structure Refinement

compound	1	2
empirical formula	C ₃₆ H ₃₆ BaCl ₂ N ₄ Ni ₂ O ₁₃	C ₃₂ H ₃₂ Cl ₂ N ₄ Ni ₃ O ₁₄
fw	1058.35	943.64
temp, K	293(2)	173(2)
wavelength, Å	0.71073	0.71073
cryst syst, space group	monoclinic, <i>P</i> 2 ₁ / <i>c</i> (no. 14)	monoclinic, <i>C</i> 2/ <i>c</i> (no. 15)
unit cell dimensions		
<i>a</i> , Å	10.995(2)	10.3020(15)
<i>b</i> , Å	20.830(4)	21.818(3)
<i>c</i> , Å	19.567(4)	17.796(4)
β , deg	116.94(3)	118.98(2)
vol, Å ³	3995(1)	3499(1)
<i>Z</i>	4	4
ρ_{calc} , Mg/m ³	1.760	1.791
μ , mm ⁻¹	2.111	1.828
no. of data/restraints/ params	4575/0/258	3085/0/241
$R(F_o)^a$ [$I > 2\sigma(I)$]	0.0766	0.0650
$R_w(F_o^2)^a$ [$I > 2\sigma(I)$]	0.1502	0.1396

^a $R(F_o) = \sum ||F_o| - |F_c|| / \sum |F_o|$; $R_w(F_o^2) = [\sum (w(F_o^2 - F_c^2)^2) / \sum (w(F_o^2)^2)]^{1/2}$; $w = 1/[\sigma^2(F_o^2) + (AQ)^2 + BQ]$ where $Q = [\max(F_o^2, 0) + 2F_c^2]/3$.

measurements, to control the absence of decay and the equipment stability. Data reductions have been made by means of the XSCANS¹⁷ program.

Crystal Structure Determination of $\{[Ni(\text{salen})]_2\text{Ba}(\text{ClO}_4)_2(\text{thf})\}$ (1). The crystals of $\{[Ni(\text{salen})]_2\text{Ba}(\text{ClO}_4)_2(\text{thf})\}$ are ruby-red monoclinic prisms. One of them, of dimensions $0.24 \times 0.20 \times 0.02$ mm, was mounted on the diffractometer at room temperature, and the cell parameters are listed in the second column of Table 1. The diffraction symmetry and systematic absences indicated the *P*2₁/*c* space group. A redundant set of data was collected by measuring between $\theta = 2.08^\circ$ and $\theta = 22.0^\circ$ in the range $-1 \leq h \leq 11$, $-1 \leq k \leq 21$, and $-20 \leq l \leq 19$. A total of 5839 reflections were measured, corrected for Lorentz and polarization effects and for absorption by using the ψ -scan method and obtaining 0.6777 and 0.9909 as the minimum and the maximum transmission factors. After the equivalents ($R_{\text{int}} = [\sum |F_o^2 - F_o^2(\text{mean})| / \sum |F_o^2|] = 0.0704$) were merged, a set of 4575 unique reflections was obtained. The structure was solved by the automatic statistical procedure contained in the SHELXTL¹⁸ program and was refined by the least-squares method contained in the same program. The high values of thermal parameters of some peripheral atoms of perchlorate and thf ligands probably indicate the presence of some degree of disorder in these groups. As it was impossible to obtain crystals of better quality, in the final refinement cycles only Ba, Ni, and Cl atoms were refined with anisotropic thermal factors. The hydrogen atoms were introduced in calculated positions and during the refinement were allowed to ride on the connected carbon atoms. The final reliability factors are listed in Table 1.

Crystal Structure Determination of $\{[Ni(\text{salen})]_2\text{Ni}(\text{H}_2\text{O})_2(\text{ClO}_4)_2\}$ (2). A monoclinic prismatic shaped ruby-red crystal of $\{[Ni(\text{salen})]_2\text{Ni}(\text{H}_2\text{O})_2(\text{ClO}_4)_2\}$, with dimensions $0.28 \times 0.14 \times 0.07$ mm, was selected for diffractometric study. To reduce the thermal motion and the effects of a dynamic disorder, eventually present, the temperature was lowered to 173 K and the lattice parameters listed in Table 1 were observed. The diffraction symmetry and systematic absences suggested *C*2/*c* or *Cc* as the possible space groups. The intensity data were collected measuring between $\theta = 3.22^\circ$ and $\theta = 25.0^\circ$ in the range $-7 \leq h \leq 12$, $-1 \leq k \leq 25$, and $-21 \leq l \leq 19$. A total of 3945 reflections were collected, corrected for Lorentz and polarization effects and for absorption by using the ψ -scan method and obtaining 0.201 and 0.892 as the minimum and the maximum transmission factors. After the equivalents ($R_{\text{int}} = 0.0573$) were merged, a set of 3085 of unique reflections was obtained. The structure was solved in the centrosym-

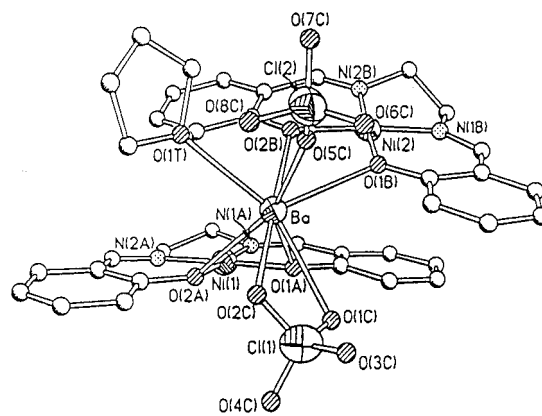


Figure 1. View of the molecular structure of $\{[Ni(\text{salen})]_2\text{Ba}(\text{ClO}_4)_2(\text{thf})\}$ (1). Ba, Ni, and Cl atoms are represented by thermal ellipsoids at 50% probability. C, N, and O atoms are represented by the spheres of arbitrary radii. Hydrogen atoms have been omitted. Only one of the two limit positions of the disordered perchlorate group facing Ni(1) is shown.

metric space group by the statistical procedure contained in the SHELXTL¹⁸ program.

Notwithstanding the low temperature (173 K) used in data collection, some of the anion maxima on the Fourier synthesis appear to be too large for representing the real thermal motion of their atoms. Moreover, the centroids of the maxima around Cl(2) (0, *y*, 1/4) did not respect the normal tetrahedral geometry of the perchlorate. This behavior has been considered as the result of a statistical distribution of the involved perchlorate in two different positions, symmetrically disposed around the 2-fold axis, close to each other and sharing the positions of two oxygen atoms involved in the hydrogen bonding. Two different ClO_4^- groups with fixed geometry and half-occupancy and partially superimposed were then introduced instead of perchlorate(2), while the atoms of perchlorate(1), which show a more correct geometry, were allowed to refine independently. The hydrogens of water molecules were introduced in calculations as found in the difference Fourier synthesis and not refined. The other hydrogen atoms were introduced in calculated positions and allowed to ride during the refinement on the connected carbon atoms.

The final refinement cycle of this model, using anisotropic thermal factors for all the heavy atoms less those of disordered perchlorate(2), gave the reliability factors listed in the last column of Table 1.

Results and Discussion

Crystal Structures. The molecular structure of **1** is shown in Figure 1. Bond distances and angles around the metal atoms are listed in Table 2. The barium cation is coordinated to eight oxygen atoms disposed in a distorted square antiprismatic geometry. The Ba–O distances range between 2.70 and 2.84 Å. Four of the coordinated oxygen atoms belong to two Ni(salen) moieties that chelate the alkaline earth cation disposed in two almost parallel planes (dihedral angle 17.0°). As can be seen in the figure the $\{[Ni(\text{salen})]_2\text{Ba}\}^{2+}$ moiety shows an approximate *C*₂ symmetry. The quasi-2-fold axial symmetry is broken, however, by the other ligands, thf and perchlorate, completing the eight coordination of barium.

The ClO_4^- groups, notwithstanding their very weak basicity, are brought into the coordination sphere of the cation by the opposite charge and by the absence of competing ligands, one of them binding to barium as a bidentate ligand. The $[Ni(\text{salen})]$ groups show their usual geometry¹⁹ with the square-planar nickel, with only a slight lengthening of the Ni–O (av 1.86 Å) as result of the lowered electron density of the oxygen upon

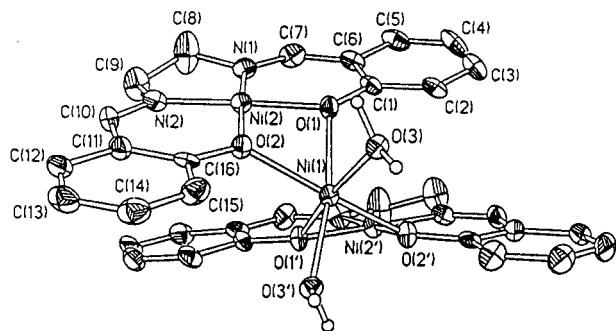
(17) XSCANS, X-ray Single Crystal Analysis System, rel. 2.1, Siemens Analytical X-ray Instruments Inc., Madison, WI, 1994.

(18) Sheldrick, G. M. SHELXTL-Plus, rel. 5.03, Siemens Analytical X-ray Instruments Inc., Madison, WI, 1994.

(19) Shkol'nikova, L. M.; Yumal', E. M.; Shugam, E. A.; Voblikova, V. A. *Zh. Strukt. Khim.* **1970**, *11*, 886.

Table 2. Bond Lengths (Å) and Angles (deg) around the Metals in the Molecular Structure of **1**

Ba—O(1B)	2.696(11)	Ba···Ni(2)	3.703(3)
Ba—O(2A)	2.745(10)	Ni(1)—N(1A)	1.833(14)
Ba—O(1A)	2.744(10)	Ni(1)—N(2A)	1.850(13)
Ba—O(1T)	2.752(13)	Ni(1)—O(2A)	1.860(11)
Ba—O(2B)	2.756(12)	Ni(1)—O(1A)	1.866(10)
Ba—O(5C)	2.78(2)	Ni(2)—N(2B)	1.840(16)
Ba—O(2C)	2.838(16)	Ni(2)—O(1B)	1.853(11)
Ba—O(1C)	2.842(13)	Ni(2)—N(1B)	1.863(16)
Ba···Ni(1)	3.557(3)	Ni(2)—O(2B)	1.866(11)
O(1B)—Ba—O(2A)	134.2(3)	O(5C)—Ba—O(2C)	74.7(5)
O(1B)—Ba—O(1A)	81.1(3)	O(1B)—Ba—O(1C)	88.7(4)
O(2A)—Ba—O(1A)	54.2(3)	O(2A)—Ba—O(1C)	87.2(3)
O(1B)—Ba—O(1T)	119.4(4)	O(1A)—Ba—O(1C)	72.7(3)
O(2A)—Ba—O(1T)	88.4(4)	O(1T)—Ba—O(1C)	143.2(4)
O(1A)—Ba—O(1T)	131.0(3)	O(2B)—Ba—O(1C)	134.9(4)
O(1B)—Ba—O(2B)	56.4(3)	O(5C)—Ba—O(1C)	97.9(5)
O(2A)—Ba—O(2B)	97.6(3)	O(2C)—Ba—O(1C)	47.6(4)
O(1A)—Ba—O(2B)	74.3(3)	N(1A)—Ni(1)—N(2A)	86.3(6)
O(1T)—Ba—O(2B)	81.8(4)	N(1A)—Ni(1)—O(2A)	176.7(5)
O(1B)—Ba—O(5C)	75.9(5)	N(2A)—Ni(1)—O(2A)	94.3(6)
O(2A)—Ba—O(5C)	149.8(5)	N(1A)—Ni(1)—O(1A)	95.0(5)
O(1A)—Ba—O(5C)	155.4(5)	N(2A)—Ni(1)—O(1A)	178.6(6)
O(1T)—Ba—O(5C)	69.7(5)	O(2A)—Ni(1)—O(1A)	84.4(5)
O(2B)—Ba—O(5C)	99.6(5)	N(2B)—Ni(2)—O(1B)	174.5(6)
O(1B)—Ba—O(2C)	121.3(4)	N(2B)—Ni(2)—N(1B)	83.9(7)
O(2A)—Ba—O(2C)	87.5(4)	O(1B)—Ni(2)—N(1B)	94.8(6)
O(1A)—Ba—O(2C)	111.0(4)	N(2B)—Ni(2)—O(2B)	94.1(6)
O(1T)—Ba—O(2C)	95.8(4)	O(1B)—Ni(2)—O(2B)	87.7(5)
O(2B)—Ba—O(2C)	174.2(4)	N(1B)—Ni(2)—O(2B)	174.2(6)

**Figure 2.** Molecular structure of the cation $[\{\text{Ni}(\text{salen})\}_2\text{Ni}(\text{H}_2\text{O})_2]^{2+}$ (**2**). Thermal ellipsoids are at 30% probability. Only the hydrogen atoms of the water ligand are represented for clarity. The apex in the atom labels has the same meaning as in Table 2.

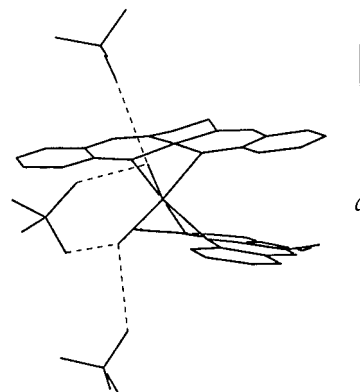
coordination, similar to that found in the addition complex between $[\text{Ni}(\text{salen})]$ and sodium.²⁰ The molecules of **1** are held together in the crystal by van der Waals interactions.

The crystal structure of **2** is made by separated cations $[\{\text{Ni}(\text{salen})\}_2\text{Ni}(\text{H}_2\text{O})_2]^{2+}$ and anions ClO_4^- . The molecular structure of a cation is shown in Figure 2. Bond distances and angles around the metals are listed in Table 2. Two $\text{Ni}(\text{salen})$ groups chelate with their oxygen atoms to $\text{Ni}(1)$ ion, which completes its coordination by linking two water molecules. The coordination geometry is distorted octahedral with $\text{Ni}-\text{O}$ distances ranging between 2.046 and 2.096 Å. The rigid closeness of the bite of $\text{Ni}(\text{salen})$ as bidentate ligand is the main cause of distortion ($\text{O}(1)-\text{Ni}(1)-\text{O}(2)$ angle = 71.6°). The cation possesses crystallographic C_2 symmetry with the 2-fold axis passing through the $\text{Ni}(1)$ atom. The $\text{Ni}(\text{salen})$ planes are disposed at the same dihedral angle (17.6°) as in compound **1**.

Table 3. Bond Lengths (Å) and Angles (deg) around the Metals in the Molecular Structure of **2**^a

Ni(1)—O(3)	2.046(5)	Ni(2)—N(1)	1.823(6)
Ni(1)—O(1)	2.096(5)	Ni(2)—N(2)	1.832(7)
Ni(1)—O(2)	2.070(5)	Ni(2)—O(2)	1.858(5)
Ni(1)···Ni(2)	2.923(1)	Ni(2)—O(1)	1.858(5)
O(3)—Ni(1)—O(3')	96.2(3)	O(1)—Ni(1)—O(1')	88.5(3)
O(3)—Ni(1)—O(2')	99.7(2)	N(1)—Ni(2)—N(2)	86.6(3)
O(3)—Ni(1)—O(2)	90.1(2)	N(1)—Ni(2)—O(2)	176.5(3)
O(2)—Ni(1)—O(2')	165.4(3)	N(2)—Ni(2)—O(2)	95.7(2)
O(3)—Ni(1)—O(1')	170.3(2)	N(1)—Ni(2)—O(1)	95.7(3)
O(2)—Ni(1)—O(1')	97.6(2)	N(2)—Ni(2)—O(1)	177.5(3)
O(3)—Ni(1)—O(1)	88.3(2)	O(2)—Ni(2)—O(1)	82.0(2)
O(2)—Ni(1)—O(1)	71.6(2)		

^a The primes indicate $-x + 1, y, -z + 1/2$.

**Figure 3.** Scheme of hydrogen interactions among the cations and the anions in the crystal structure of **2**. The infinite columns grow along *a*.

In the crystal structure of **2**, the ions, besides the normal electrostatic interactions, are held together also by the large number of hydrogen bonds the water molecules make with the perchlorate anions. As shown in Figure 3 each cation is connected by two hydrogen bonds to the disordered perchlorate group placed in front of them and sharing axis 2. It links, moreover, two other ClO_4^- groups placed on the neighboring axis 2 spanned by *a*. Infinite chains growing along *a* are so built.

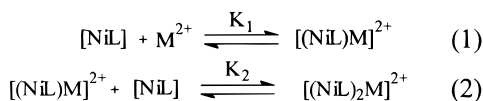
The formation of the adducts was confirmed by the appearance of IR bands in the region of absorption of perchlorate ion¹³ (1000 cm^{-1}). Moreover, the stretching frequency of the $\text{C}=\text{N}$ bond shifted from 1629 to about 1624 cm^{-1} upon formation of the adducts. The $\text{C}-\text{O}$ stretching frequencies are at about 1550 cm^{-1} , while for the free $[\text{Ni}(\text{salen})]$ ligand this absorption band is at 1532 cm^{-1} . The same increase was found for alkali metal— $[\text{Ni}(\text{salen})]$ adducts.^{8b}

Equilibria in Solution. The study of the equilibria in acetonitrile solution between the mononuclear²¹ nickel complexes and metal ions M^{2+} was performed, observing the spectral changes in the UV—vis region induced by adding increasing amounts of $\text{M}(\text{ClO}_4)_2$. In fact, alkali and alkaline earth cations can induce remarkable modifications on the electronic absorption spectra of O-ligands (metal-coordinated or not) in solution. Such spectral perturbations are generally recognized to arise from cation—ligand binding. The associated interaction energy is commonly attributed to an electrostatic term due to ion—dipole interaction, to a polarization term arising from ion-induced dipole interaction, and/or to a charge-transfer term. In the metal

(20) Bresciani-Pahor, N.; Calligaris, M.; Delise, P.; Nardin, G.; Randaccio, L.; Zotti, E.; Fachinetti, G.; Floriani, C. *J. Chem. Soc., Dalton Trans.* **1976**, 2310.

(21) Holm, R. H.; Everett, G. W., Jr.; Chakravorty, A. In *Progress In Inorganic Chemistry*; Cotton, F. A., Ed.; Interscience Publishers: New York, 1966; Vol 7, pp 130–150.

Scheme 1



ion–base association, the electrostatic term predominates. On this basis we expected alkaline earth cations to give stronger interactions with the nickel(II) complexes than the cations of group I, and to determine more remarkable spectral changes, both being phenomena correlated with the density of charge of the metal M. Moreover, the cation M^{2+} should have been able to exhibit stronger aggregating properties, involving more than one molecule of the complex in solution, as in the solid state. In fact adducts of type $2[\text{NiL}] \cdot \text{M}(\text{ClO}_4)_2$ were isolated from tetrahydrofuran. Two of them, $[\{\text{Ni}(\text{salen})\}_2\text{Ba}(\text{ClO}_4)_2(\text{thf})]$ and $[\{\text{Ni}(\text{salen})\}_2\text{Ni}(\text{H}_2\text{O})_2](\text{ClO}_4)_2$, were obtained as crystalline solids suitable for X-ray analysis (see above). On the contrary, no adducts of 1:1 stoichiometry could be isolated. In solution a greater complexity of the systems under investigation was observed.

Significant changes of the spectra of the $[\text{NiL}]$ complexes took place in the UV–vis region (between 300 and 480 nm) of MLCT and $\pi \rightarrow \pi^*$ absorption bands,²² by adding $\text{M}(\text{ClO}_4)_2$. The collected spectroscopic data were subjected to a multi-wavelength analysis, leading to the formulation of the set of equilibria given in Scheme 1, where for clarity the solvent molecules are omitted. Other plausible schemes were also tested as alternatives to Scheme 1. The criterion of choice was that of rejecting, among the models of comparable standard deviation, those which led to the existence of species in concentration too low (less than 2%) to have any significance, gave no good fits at all the wavelengths (up to 25), and/or gave unreasonable calculated spectra for some species involved in the equilibria. For instance, the simplest ones, involving only the adduct of 1:1 or 2:1 stoichiometry, were not found to satisfy such essential requirements.

Equilibrium 1 results in the formation of the chelate–adduct $[(\text{NiL})\text{M}]^{2+}$ of 1:1 complex-to-metal molar ratio, analogous to that one involving alkali metal ions.⁷ In equilibrium 2, another molecule of the complex acts as an additive O_2 donor set, substituting two other molecules of solvent in the coordination sphere of the metal M^{2+} . The resulting product is a trinuclear complex with the metal M^{2+} surrounded by two $[\text{NiL}]$ units.

Figure 4a shows a set of spectra recorded in acetonitrile for the $[\text{Ni}(\text{salen})]/\text{Ba}(\text{ClO}_4)_2$ system, which is representative of the increasing hypsochromic shift observed, with respect to the starting $[\text{NiL}]$ spectrum, upon addition of increasing amounts of $\text{M}(\text{ClO}_4)_2$. Similar, but less remarkable, shifts have also been found⁷ for alkali cations and ascribed to a greater destabilization of the electronic ground state of the $[\text{NiL}]$ complex with respect to the excited one, determined by the interacting cation M^+ .

Calculated spectra of the $[(\text{NiL})_2\text{M}]^{2+}$ and $[(\text{NiL})\text{M}]^{2+}$ adducts were very similar in shape as is shown, for example, in Figure 4b for $[\text{NiL}] = [\text{Ni}(\text{salen})]$. Their absorption maxima are shifted differently with respect to that of the starting complex, the $[(\text{NiL})\text{M}]^{2+}$ adduct having the largest hypsochromic shift. The difference between the two adducts of Scheme 1 is greater for $\text{M}^{2+} = \text{Ba}^{2+}$ and decreases with decreasing alkaline earth metal ion size. The $[(\text{NiL})_2\text{M}]^{2+}$ adduct has molar absorptivities about 2-fold greater than those of $[(\text{NiL})\text{M}]^{2+}$, in agreement with the

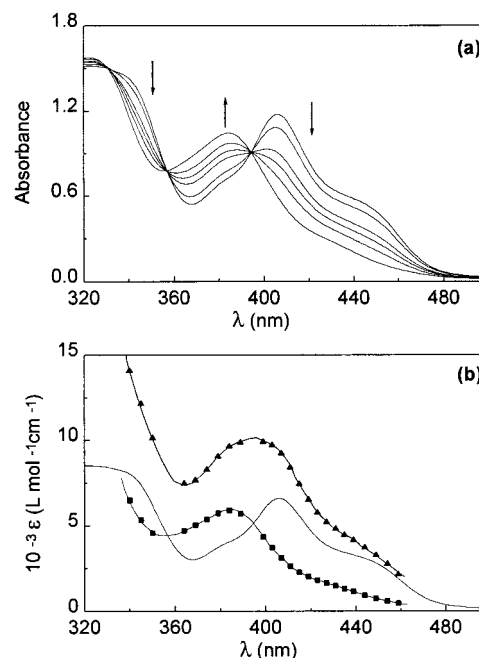


Figure 4. (a) Changes in the absorption spectrum of a $[\text{Ni}(\text{salen})]$ acetonitrile solution ($1.80 \times 10^{-4} \text{ mol L}^{-1}$) with increasing $\text{Ba}(\text{ClO}_4)_2$ concentration (0 – $5.33 \times 10^{-2} \text{ mol L}^{-1}$). Optical path 1 cm. (b) Experimental absorption spectrum of $[\text{Ni}(\text{salen})]$ (solid line) and calculated absorption spectra of $[\text{Ni}(\text{salen})\text{Ba}]^{2+}$ (■) and $[\{\text{Ni}(\text{salen})\}_2\text{Ba}]^{2+}$ (▲) adducts in acetonitrile.

presence in the molecule of an additional equivalent chromophore center.

Data analysis on spectroscopic measurements for the $[\text{Ni}(\text{salen})]/\text{Ba}(\text{ClO}_4)_2$ system in thf confirmed that the equilibria and the species involved were identical to those found in acetonitrile. Moreover, no remarkable changes in the position of the absorption maxima of the adducts were observed when thf was used as solvent instead of acetonitrile, confirming the electrostatic nature of the interaction between host–guest moieties without interposition of solvent molecules, as was found for alkali cations.⁷

Calculated λ_{max} values of $[\{\text{Ni}(\text{salen})\}_2\text{M}]^{2+}$ and $[\text{Ni}(\text{salen})]^{n+}$ ($n = 1, 2$) adducts are reported in Table 4. They have to be considered only approximate estimations for $\text{M}^{n+} = \text{Cs}^+$ and Mg^{2+} . The former ion gives rise to a very weak equilibrium with the starting complex $[\text{ML}]$, so that quantitative evaluation of K_1 and of the other parameters inherent to the equilibrium as λ_{max} was only approximate. For opposite reasons, such an evaluation was even inadequate for $\text{M}^{2+} = \text{Mg}^{2+}$ whose equilibria 1 and 2 (Scheme 1) were found strongly shifted toward the right. In this case the λ_{max} of the experimental spectrum recorded after addition of an excess of magnesium salt was considered a reasonable estimation of the λ_{max} value for the $[\text{Ni}(\text{salen})\text{Mg}]^{2+}$ adduct. In fact in these experimental conditions the concentration of the starting complex should be negligible and the two adducts should have close absorption maxima, on the basis of the considerations pointed above for the adducts of the other cations M^{2+} .

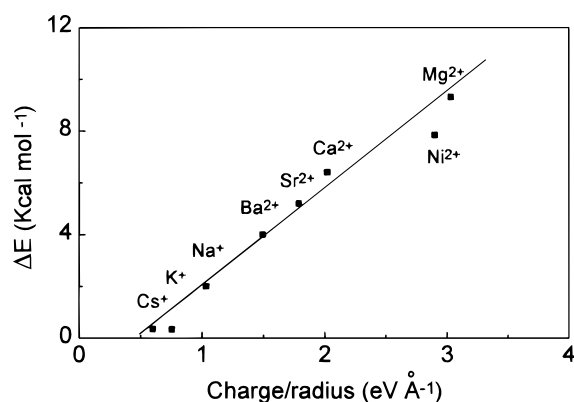
With these assumptions, a good correlation was found between $\Delta\lambda_{\text{max}}$ expressed as $\Delta\epsilon$, calculated for the $[\text{Ni}(\text{salen})\text{M}]^{n+}$ adduct, and the charge/radius ratio of all the cations under examination (Figure 5).

Also for the $[\text{Ni}(\text{salpren})]/\text{M}(\text{ClO}_4)_2$ systems, when $\text{M}^{2+} = \text{Sr}^{2+}$, Ca^{2+} , and Mg^{2+} , the equilibrium constants were too great to be evaluated ($\log(K_1K_2) > 8$). An analogous approximate

Table 4. Calculated λ_{\max} (nm) of $[\text{Ni}(\text{salen})\text{M}]^{n+}$ ($n = 1, 2$) and $\{[\text{Ni}(\text{salen})\}_2\text{M}\}^{2+}$ Adducts in Acetonitrile at 25 °C and log Values of the Stability Constants of $[\text{NiL}]\text{M}^{n+}$ ($n = 1, 2$) and $[\text{NiL}_2]\text{M}^{2+}$ Adducts According to Scheme 1 in Acetonitrile at 25 °C

[NiL]	M ²⁺ or M ⁺ salt	log K ₁	λ_{\max}^a	log K ₂	λ_{\max}^b	log(K ₂ /K ₁)
[Ni(salphen)]	NaBPh ₄	1.87 ^c				
	Ba(ClO ₄) ₂	2.45 ± 0.04		4.05 ± 0.04		1.60 ± 0.06
	Sr(ClO ₄) ₂	2.49 ± 0.09		4.08 ± 0.07		1.6 ± 0.1
	Ca(ClO ₄) ₂	3.0 ± 0.15		4.21 ± 0.03		1.2 ± 0.15
	Mg(ClO ₄) ₂	2.8 ± 0.2		4.9 ± 0.1		2.1 ± 0.2
	[Ni(CH ₃ CN) ₆](ClO ₄) ₂	1.3 ± 0.15		3.70 ± 0.08		2.4 ± 0.2
[Ni(salen)] ^h	CsBPh ₄	~0.70 ^c	406 ^c			
	KBPh ₄	1.11 ^c	405 ^c			
	NaBPh ₄	1.99 ^c	396 ^c			
	Ba(ClO ₄) ₂	3.09 ± 0.02	384	3.53 ± 0.05	392	0.44 ± 0.05
	Ba(ClO ₄) ₂	2.16 ± 0.03 ^d	387 ^d	2.91 ± 0.02 ^d	390 ^d	0.75 ± 0.03
	Sr(ClO ₄) ₂	3.13 ± 0.03	378	3.72 ± 0.01	386	0.59 ± 0.03
	Ca(ClO ₄) ₂	3.8 ± 0.2	372	4.08 ± 0.04	373	0.28 ± 0.2
	Mg(ClO ₄) ₂	~6.0 ^e	359 ^f	~5.1 ^e	359 ^f	~0
	[Ni(CH ₃ CN) ₆](ClO ₄) ₂	2.40 ± 0.06	365	3.91 ± 0.04	370	1.51 ± 0.07
	[Ni(salpren)] ^g	Ba(ClO ₄) ₂	3.68 ± 0.05		3.59 ± 0.02	
	[Ni(CH ₃ CN) ₆](ClO ₄) ₂	2.51 ± 0.07		3.0 ± 0.10		0.5 ± 0.1

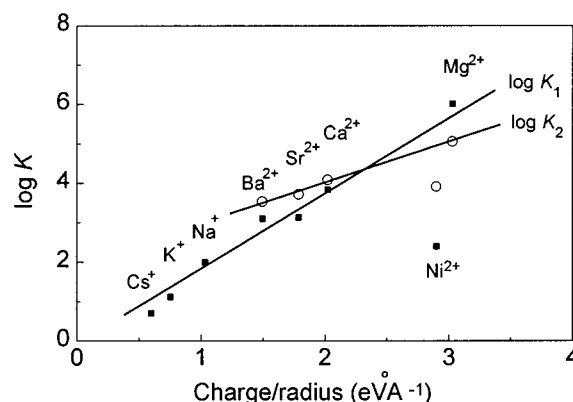
^{a,b} Calculated λ_{\max} of (a) $[\text{Ni}(\text{salen})\text{M}]^{n+}$ ($n = 1, 2$) and (b) $\{[\text{Ni}(\text{salen})\}_2\text{M}\}^{2+}$ adducts in acetonitrile at 25 °C. ^c From ref 7. ^d In thf. ^e Values extrapolated from the plot of log K₁ or log K₂ vs charge/ionic radius ratio for the other cations. ^f Extrapolated from experimental spectra. ^g Equilibrium constants with Sr(ClO₄)₂, Ca(ClO₄)₂, and Mg(ClO₄)₂ were too great to be determined (log(K₁K₂) > 8). ^h For [Ni(salen)] $\lambda_{\max} = 407$ nm in acetonitrile and $\lambda_{\max} = 417$ nm in thf.

**Figure 5.** $\Delta E = \Delta(h\nu)$ (kcal mol⁻¹) (calculated on the basis of the data of Table 4) against charge/radius of Mⁿ⁺ for $[\text{Ni}(\text{salen})\text{M}]^{n+}$ adducts ($n = 1, 2$).

estimation of λ_{\max} was obtained from the experimental spectra recorded in the presence of an excess of perchlorate. The hypsochromic shift with respect to the $[\text{Ni}(\text{salpren})]$ spectrum ($\lambda_{\max} = 412$ nm) ranges from 340 to 346 nm²³ with a general flatness of the effects produced by different M²⁺ cations, holding a regular trend along the series of the alkaline earth cations as well. This behavior reflects the greater coordinating capability of the $[\text{Ni}(\text{salpren})]$ ligand, which not only gives rise to more stable adducts but also might be able to compensate the differences which might arise from changes in the cation dimensions.

Finally, for the $[\text{Ni}(\text{salphen})]/\text{M}(\text{ClO}_4)_2$ systems, the absorption maxima of the adducts fall in a UV-vis region of small changes of the spectra and hence are not suitable for the calculation of the molar absorptivities of the species involved in the equilibria.

The logarithms of the stability constants related to Scheme 1 are reported in Table 4. A common feature of all the cations examined is that log K₂ values are all greater than log K₁, denoting a trend inverse to that usually found for the stepwise formation of complexes from free ligands.²⁴

**Figure 6.** log K₁ (■) and log K₂ (○) (Scheme 1) against charge/radius of M²⁺ and M⁺ for $[\text{Ni}(\text{salen})]/\text{M}^{n+}$ adducts.

As a general rule, it can be noted that the stability constants for the series of alkali and alkaline earth cations increase with increasing charge/ionic radius ratio. As shown in Figure 6 for the $[\text{Ni}(\text{salen})]$ adducts, log K₁ and log K₂ values are linearly proportional to the charge/ionic radius ratio. Evidently, this system lacks a preformed hole of fixed size such as that offered, for instance, by crown ethers,¹ so that the charge density of the metal M, rather than its dimensions, becomes the main factor in determining the stability of the adduct. On the contrary, in the case of the $[\text{Ni}(\text{salphen})]$ systems, where more constraints are imposed by its geometry,²⁵ there is a marked maximum in log K₁ with Ca²⁺.

From the comparison among different nickel complexes, it can be noted that the log K₁ values increase when the bridge skeleton between the two nitrogen atoms confers a greater flexibility to the whole complex. Thus, the stability constants of the adducts of Sr²⁺, Ca²⁺, and Mg²⁺ with the more flexible²⁶ $[\text{Ni}(\text{salpren})]$ complex were too great to be evaluated. On the other hand, it is evident that the values of log(K₂/K₁), which are related to the formation of the 2:1 adducts starting from M²⁺ and the 1:1 adducts, increase with the structural rigidity of the [NiL] complex, denoting that this factor may act in two

(23) λ_{\max} (nm) = 341 for Ni²⁺, 340 for Mg²⁺, 344 for Ca²⁺, and 346 for Ba²⁺.

(24) Burgess, J. *Ion In Solutions*; Ellis Horwood Ltd.: Chichester, England, 1988; Chapter 6.

(25) Biradar, N. S.; Kulkarni, V. H. *J. Inorg. Nucl. Chem.* **1971**, *33*, 2451.

(26) Mockler, G. M.; Chaffery, G. W.; Sinn, E.; Wong H. *Inorg. Chem.* **1972**, *11*, 1308.

opposite ways. Rigidity inhibits the ligand in adjusting its geometrical disposition as a function of the guest metal dimensions. The same rigidity might be important to create a hosting cage, constituted by two units of the [NiL] ligand, in which the guest metal is shielded more efficiently with respect to competitive solvent coordination.

Finally, Ni²⁺ forms adducts less stable than those of the alkaline earth cations. This occurrence, apparently in contrast with the low value of its radius (0.72 Å), confirms the softer acidic character of nickel with respect to group II cations and, hence, its lower affinity toward hard Lewis O-bases.

Acknowledgment. The investigations were supported in part by CNR and by MURST. We thank Dr. Augusto Lupetti for the plasma and ionic chromatographic analysis.

Supporting Information Available: Experimental and calculated spectra for the ([Ni(salphen)]/Ca(ClO₄)₂) system and two X-ray crystallographic files, in CIF format. This material is available free of charge via the Internet at <http://pubs.acs.org>.

IC990189J